Available online at www.sciencedirect.com
SCIENCE DIRECT®
Thermochimica Acta 412 (2004) 113–119
thermochimica acta
www.elsevier.com/locate/tca

Gas renewal in the horizontal furnace of a thermobalance

Chandana Rath, J. Farjas, P. Roura*

GRMT, Departament de Física, Universitat de Girona, Campus Montilivi, Edif. PII, E17071 Girona, Catalonia, Spain

Received 25 March 2003; received in revised form 11 September 2003; accepted 11 September 2003

Abstract

The time delay needed to renew the atmosphere inside the furnace of a thermogravimeter is a key parameter while studying the very early stages of chemical reactions involving a reactive gas. In this paper, we report the time evolution of oxygen partial pressure in a cylindrical horizontal furnace. The measurements have been carried out by means of the oxidation of nickel microparticles. The time that oxygen needs to reach the sample's position has been measured as a function of the furnace temperature and of gas flow rate. The values of time delay are shorter than expected at low flow rates due to gas interdiffusion, whereas are higher than expected at high flow rates due to partial thermalisation of gas. Gas interdiffusion has been computed by solving the mass transport equation in one dimension and selecting a suitable boundary condition at the end of the furnace. This boundary condition takes into account the abrupt reduction of section when gas flows through the exhausting hose.
© 2003 Elsevier B.V. All rights reserved.

Keywords: Gas renewal; Horizontal furnace; Thermogravimeter; Gas diffusion; Thermalisation

1. Introduction

In experiments involving chemical reactions with gases, the time required to renew the atmosphere can be crucial. For instance, the information concerning the first stages of oxidation of Si [1] or SiC [2] at high temperature (say >900 °C) may be lost if the mass gain curve could not be measured in steady conditions (constant temperature and oxygen partial pressure) for times shorter than a few minutes. Although the oxidation rate can be slowed down simply by diminishing the oxygen partial pressure, the dominating oxidation mechanisms may not be the same at low pressure [3]. So, it is worth analysing the conditions that best reduce the time needed to replace the inert atmosphere around the sample by the reactive gas.

In this paper, we report the dependence of the time elapsed for gas renewal on gas flow rate and temperature. Systematic experiments have been carried out to understand gas renewal behaviour inside the horizontal furnace of a thermobalance.

2. Experiment

Experiments have been performed in a Mettler Toledo (SDTA 851^e LF) thermobalance. Fig. 1 contains the scheme of its horizontal furnace, where the main geometrical parameters, sample location and "reactive" and "protective" gas inlets are shown. Just below the sample holder, a thermocouple allows direct measurement of the local temperature and with a suitable calibration one can determine the sample's temperature [4].

The evolution of oxygen partial pressure has been analysed by studying Ni microparticles oxidation. Ni powders have been furnished by Goodfellow Ltd. (ref. LS219278, purity of 99.8%). These particles are irregularly shaped and their diameter range is from 3 to 7 μm. We have chosen Ni powders among a number of other powders (Nb, Cr, Fe, Cu, B, graphite, etc.) because of their oxidation kinetics. Precisely, these particles exhibit a linear kinetics that lasts for several hours. This fact can be stated from Fig. 2. After a transient, the mass gain curve shows a well-defined linear kinetics that persists during the whole measurement, i.e. 60 min. In fact, although the linear-parabolic oxidation kinetics of Ni is reported in literature [5], the linear term is already dominant for short times and the parabolic contribution is detectable only beyond several tens of hours. The oxidation rate is almost proportional to the oxygen partial

* Corresponding author. Tel.: +34-972-418383; fax: +34-972-419098.
E-mail address: pere.roura@udg.es (P. Roura).

0040-6031/$ – see front matter © 2003 Elsevier B.V. All rights reserved.
doi:10.1016/j.tca.2003.09.007

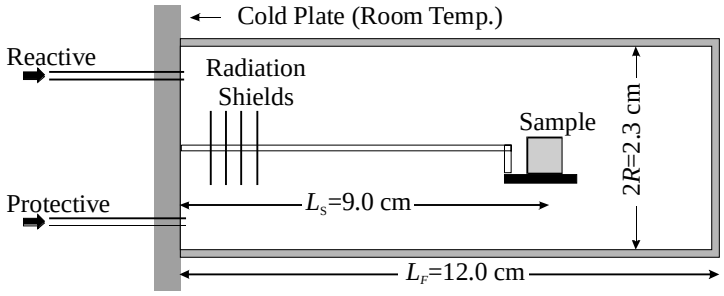

Fig. 1. Scheme of the horizontal cylindrical furnace under study.

pressure in the 0.1–1.0 atm range (Fig. 3). This dependence allows a direct calculation of oxygen partial pressure from the slope of the thermogram in the non-steady period that appears when the oxygen is turned ON (Fig. 2). Finally, no significant dependence of the oxidation rate on temperature has been observed from 600 to 1200 °C. This fact simplifies the comparison of results obtained at different temperatures.

Most of the experiments have been carried out as follows. The powder is introduced at room temperature (T_{RT}) in the furnace inside a high purity alumina crucible. Then, a constant flow of inert gas (N_2) is allowed to pass through the furnace for 10 min, subsequently the furnace is heated at 10 K min^{-1} until the programmed temperature (T) is reached. Ten minutes later, the "reactive gas" inlet is switched from inert gas to oxygen diluted in nitrogen. During the whole experiment, the total flow rate is kept at a constant value, Q, the "protective" and "reactive" flow rates are equal to $Q/2$. In this way, mechanical disturbances to the balance arm are minimised (see the blank curve of Fig. 2). The gas flow rate and composition are controlled by a set of flowing-ball flow meters or, alternatively, by an automated gas controller driven by the thermobalance software. Although the accuracy in the gas controller is higher, it introduces an extra volume that increases significantly the time necessary for oxygen to reach the sample. The approximate values of these external volumes, V_X, are detailed in Figs. 4 and 5. In the following, we will refer to the experiments with or without the gas controller as A and B, respectively.

This method allows a direct quantification of the oxygen concentration inside the furnace at the point where the sample is placed. The derivative of the mass gain curve is proportional to oxygen partial pressure and a normalisation allows us to determine the time delay necessary to reach 50% ($t_{0.5}$) or 90% ($t_{0.9}$) of oxygen concentration at the steady regime (Fig. 2).

The reliability of this method has been verified using mass spectroscopy. To that purpose, time delays measured from mass gain curves have been compared to those obtained by a mass spectrometer whose capillary collected the gas at the sample's location. Within the experimental error, both

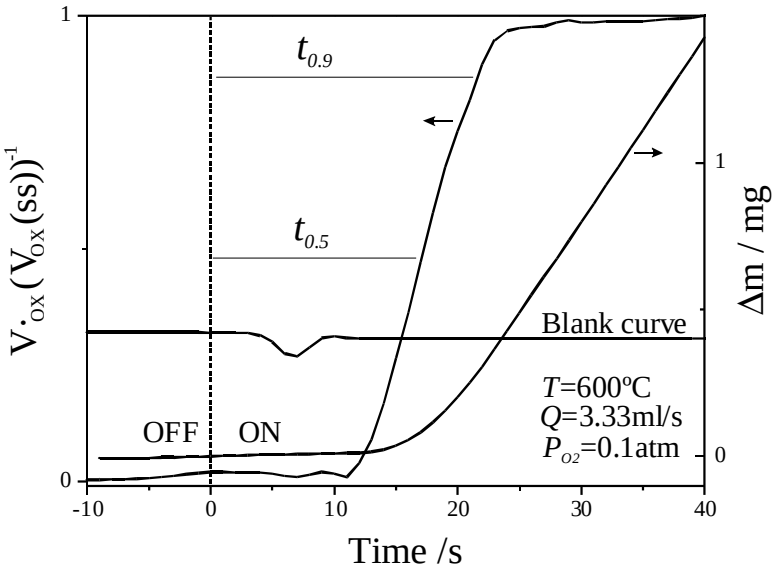

Fig. 2. Characteristic mass gain curve versus time measured in Ni microparticles. At $t = 0$ oxygen is turned ON and replaces nitrogen progressively. The blank curve, obtained with an empty crucible, has a peak due to an initial mechanical instability of the balance; the time derivative of the mass gain (V_{ox}) is almost proportional to the oxygen partial pressure (V_{ox}(ss) is the V_{ox} value at the steady state).

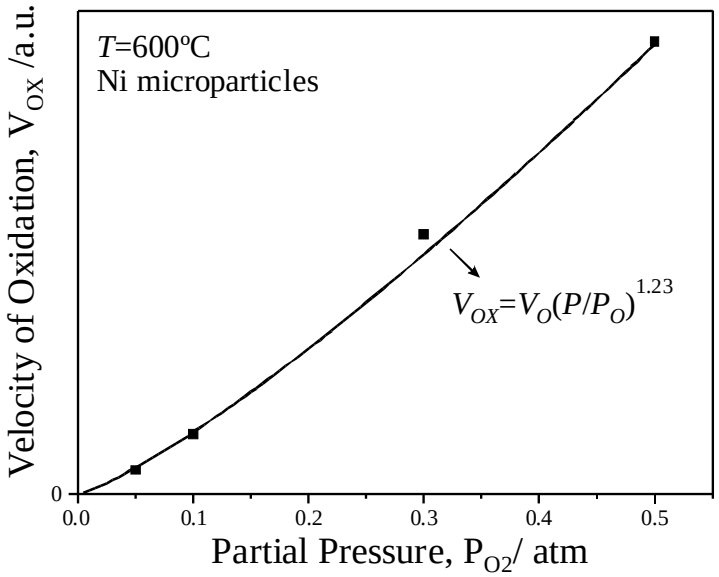

Fig. 3. Dependence of oxidation rate on oxygen partial pressure in Ni microparticles.

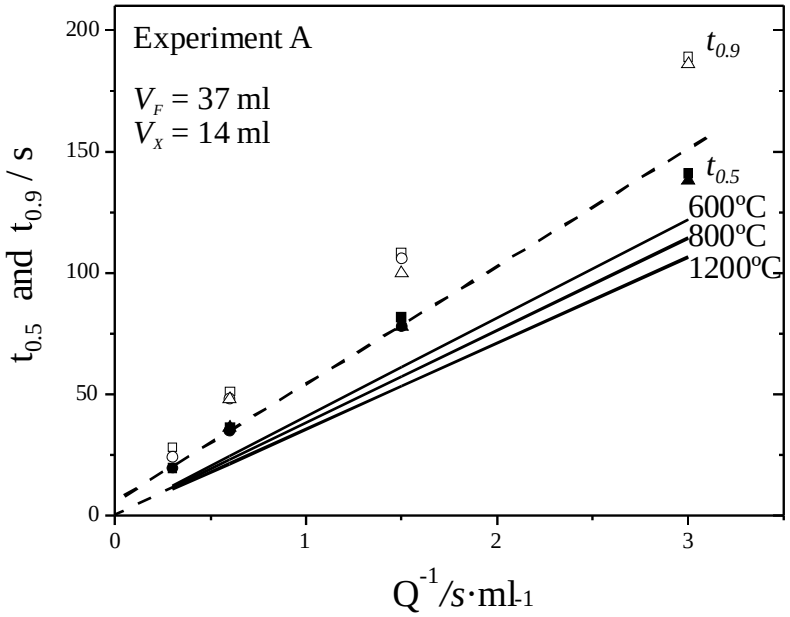

Fig. 4. Experimental time delays ($t_{0.5}$ and $t_{0.9}$) as a function of gas flow rate, Q, at 600 (squares), 800 (circles) and 1200 °C (triangles) with gas controller. Broken line: approximate linear trend of the first three flow rates. Solid lines: theoretical values at the programmed furnace temperatures.

techniques have given the same values for several flow rates and temperatures. Moreover, to ensure the technique consistency the ON–OFF and OFF–ON transients have been compared and found to be equivalent.

3. Elementary prediction of $t_{0.5}$ and comparison with experiment

A simple prediction can be obtained assuming:

(a) *One-dimensional approximation*. The oxygen concentration is a function of the axial position in the furnace or in the external hoses. Any radial dependence is neglected.

(b) *No axial diffusion*. The oxygen concentration changes abruptly from zero to its maximum value as the front of the new reactive gas passes at a given point.

(c) *Perfect gas thermalisation*. Within this context and for the rest of the paper, “gas thermalisation” means that the gas acquires the programmed temperature. We consider that at the moment where the gas enters the furnace, it thermalises instantaneously.

Within these assumptions, the time elapsed (t_D), since the oxygen is turned ON until it reaches the sample, is

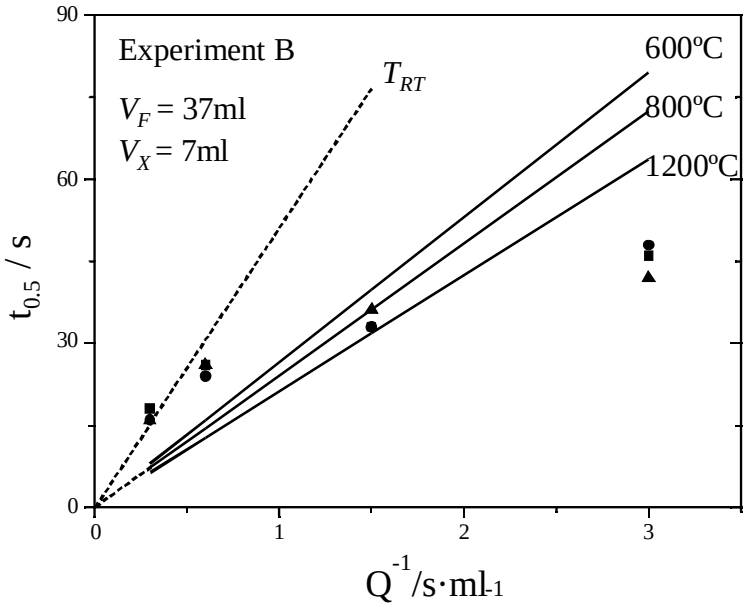

Fig. 5. Experimental time delay, $t_{0.5}$, as a function of gas flow rate, Q, in the experiments without gas controller at the same temperatures than in Fig. 4. Solid lines: expected values for perfect thermalisation. Dashed line: expected values at room temperature (no thermalisation).

equal to

$$t_D = \frac{V_F}{Q}\frac{T_{RT}}{T} + \frac{2V_X}{Q} = \left(V_F\frac{T_{RT}}{T} + 2V_X\right)Q^{-1} \quad (1)$$

where V_F and V_X are the geometrical volumes of the furnace (from the entrance to the sample's position) and the external hose, respectively; T is the programmed temperature of the furnace in K; and Q the total flow rate. The factor T_{RT}/T accounts for the expansion of the gas inside the furnace. In the calculation of the external hose contribution, Q is divided by 2 because only one-half of the gas flows through the "reactive gas" inlet. Eq. (1) predicts a proportionality relationship between t_D and $1/Q$. The proportionality constant can be interpreted as the volume of the gas, measured at room temperature, needed to replace the inert gas contained between the OFF–ON valve and the sample's position. This proportionality constant should diminish at higher furnace temperatures.

In Fig. 4, the values of $t_{0.5}$ and $t_{0.9}$, which have been obtained from the experiment with the gas controller (experiment A), have been plotted versus Q^{-1}. The flow rate values were chosen to be 20, 40 100 and 200 ml min^{-1} and the experiments have been repeated for three temperatures (600, 800 and 1200 °C). It is important to note that $t_{0.9}$ is higher than $t_{0.5}$. This indicates that oxygen does not advance like an abrupt front, it rather mixes with the inert gas in the furnace. This mixing phenomenon can be due to three effects: diffusion, the radial profile of axial velocity and turbulence, which could arise at the entrance of the furnace. Even in case where this latter effect could be neglected, quantitative analysis of the first and second effects is not simple due to the non-regular section of the furnace (i.e. radiation shields, Fig. 1) and because the mass transfer (diffusion) and momentum transfer become coupled. So, we will not make any attempt to predict the 'smoothing' of the oxygen front. Anyway, the question arises, which is the time that should be compared to t_D ($t_{0.5}$ or $t_{0.9}$)? As a first approximation, we can assume that it should be $t_{0.5}$ since it locates the average position of the oxygen front which, in principle, should not be modified by any mixing effect.

In Fig. 4, the straight lines correspond to $t_{0.5}$ calculated from Eq. (1) at three different temperatures where V_F = 37 ml and V_X = 14 ml. Several discrepancies with the experimental values of are apparent: (a) the linear relationship is not followed at the lowest flow rate (20 ml min^{-1}); (b) although the rest of the experimental points show an approximate linear behaviour, they are found at higher values than predicted from Eq. (1); and (c) no clear evolution of $t_{0.5}$ with temperature is observed. These three discrepancies could be explained through Eq. (1), simply taking into account a lack of thermalisation. Smaller values of T in Eq. (1) imply longer values of t_D. In physical terms, if the gas temperature does not reach the programmed one immediately, then the volume expansion will be smaller and more oxygen will be necessary to replace the inert gas. Consequently, $t_{0.5}$ will be longer compared to perfect thermalisation and its values at different temperatures will be closer. For the smaller flow rate, the gas needs more time to achieve the programmed temperature and $t_{0.5}$ approaches the predicted value.

4. Gas thermalisation

In this section, we will analyse the problem of thermalisation from two points of view. First, we will compare the time required for thermalisation, obtained from the energy

transport equation, against the time necessary for gas to reach the sample in its movement inside the furnace. Second, the measurement of the local temperature near the sample will reveal that the gas is cooler than the programmed temperature of the furnace and that this effect is more important at high flow rates.

Consider the ideal situation where a gas has reached thermal equilibrium with the inner walls of a cylindrical furnace of radius R. At $t = 0$, the walls are instantaneously heated to a higher temperature. Provided that the gas is transparent enough to radiation and that the temperature of the furnace walls is homogeneous, the only heating mechanism would be heat conduction and, consequently, the transient leading to thermalisation depends on the thermal diffusivity of the gas, α. This problem can be solved exactly by integrating the energy transport equation [6]. Within an error bar of 20%, the time for thermalisation, t_{th}, can be deduced to be [7]:

$$t_{th} = 0.5\frac{R^2}{\alpha} \quad (2)$$

The thermal diffusivities of oxygen and nitrogen are very similar [8]. Hence we have taken the one corresponding to air. The value of t_{th} should be compared with the fraction of t_D (Eq. (1)) corresponding to the furnace, $t_D(F)$, i.e.:

$$t_D(F) = V_F\frac{T_{RT}}{T}Q^{-1} \quad (3)$$

If $t_{th} \ll t_D(F)$, the gas thermalises just at the entrance of the furnace and, then, Eq. (1) is valid. In Table 1, the values of t_{th} and $t_D(F)$ are detailed for several flow rates and temperatures. Surprisingly, despite the general trend that indicates a higher difficulty for thermalisation at lower temperature and higher flow rates, the tabulated values predict an almost complete thermalisation under our experimental conditions. For this reason, before going further on, we will focus our attention on gas temperature.

So as to discern the gas temperature inside the furnace, we have measured the onset temperature when In and Al melt. In particular, we have analysed the local temperature measured at the sample holder, T_{local}, during heating sequences where the programmed temperature, T, was raised at a constant rate of 10 K min^{-1}. The results summarised in Table 2 show that the higher the flow rate, the higher the onset temperature is. This fact evidences that the gas flowing around the sample is cooler than the programmed temperature (i.e. it is not completely thermalised). This can be explained as follows. The crucible and holder are heated mainly by radiation [9]. So, the effect of heat exchange with the gas is less important. However, the heat exchange is more efficient with the crucible because its surface is more perpendicular to the gas stream. If the gas is cooler than the furnace walls then, at the melting onset, when the sample reaches its melting temperature, T_F, the temperature of the holder will be higher. One may think that the maximum difference of 15 K reported in Table 2 between 20 and 200 ml min^{-1}, in the case of In, means that gas thermalisation is quite good. However, as said before, the temperature is mainly determined by radiation and the gas temperature has a minor effect on the sample's temperature. This explains why the difference $T_{local} - T_F$ diminishes in the case of aluminium (Table 2), since at its melting point radiation is more intense than that at the indium melting temperature. The gas in fact, much cooler than T_{local}.

Table 1
Comparison of the thermalisation time, t_{th}, against the time required for the gas to reach the sample's position in the furnace, $t_D(F)$

Temperature (°C)	α (10^{-6} m^2 s^{-1})	$t_D(F)$ (s)		t_{th} (s)
		20 ml min^{-1}	200 ml min^{-1}	
30	20	110	11	3.3
700	170	33	3.3	0.4

Table 2
Local temperature of the sample holder at the onset of melting[a]

Metal	T_F (°C)	T_{local} (°C)		
		20 ml min^{-1}	40 ml min^{-1}	200 ml min^{-1}
In	156	153	155	168
Al	660	659	–	661

[a] 20, 40 and 200 ml min^{-1} are the Q values.

To conclude this section, we have given an experimental evidence of incomplete gas thermalisation. This contrasts with the theoretical analysis based on Eqs. (2) and (3). We think that this apparent contradiction is due to the simplicity of the model used for calculation $t_D(F)$. In fact, the radiation shields are kept at room temperature and the furnace wall temperature is not homogeneous at all. Both, radiation shields and furnace make a good thermal contact with a metallic plate located at the furnace left side (see Fig. 1) which is held at room temperature. Consequently, the time left for the gas to reach the programmed temperature, T, when it enters the furnace is much shorter than the value predicted by Eq. (3).

5. Gas interdiffusion

Despite the relative success of the lack of thermalisation in explaining the evolution of the time delay reported in Fig. 4, experiment A is not very suitable for testing whether this lack of thermalisation suffices to explain the observed behaviour or not. An important fraction of the volume that needs to be replaced by the gas is actually external to the furnace ($2V_X = 28$ ml $\approx V_F = 37$ ml) which is not temperature dependent.

The conditions of experiment B (without the gas controller and manual change of the reactive gas) are not the usual ones when carrying out routinely thermal analyses with our equipment. However, in this case, the external volume is much smaller ($2V_X = 14$ ml $\ll V_F = 37$ ml) and, consequently, the effects of thermalisation should be more

evident. We have measured $t_{0.5}$ at the same flow rates and temperatures than in experiment A. Results are plotted in Fig. 5. Now the experimental points are not aligned at all indicating, as expected, that deviations from Eq. (1) arise mainly due to processes occurring inside the furnace.

The values of $t_{0.5}$ measured at 200 ml min^{-1} (Q^{-1} = 0.3 s ml^{-1}) fall approximately in the straight line corresponding to $T = T_{RT}$ whereas the ensemble of theoretical lines (Eq. (1)) crosses the experimental values at a flow rate near 40 ml min^{-1} (Q^{-1} = 1.5 s ml^{-1}). At the lowest flow rate, in contrast with all the results of experiment A, $t_{0.5}$ is much smaller than predicted. The discrepancy with the predicted values is too big to be attributed to any experimental inaccuracy. So, an extra effect must be considered, which cannot be explained by any modification of Eq. (1). In the following, it will be shown that, at low flow rates, gas interdiffusion diminishes the time delay due to a special boundary condition that applies at the end of the furnace.

The equation governing diffusion of a gas at rest can be written [10], in one dimension, as

$$D\frac{\partial^2 c}{\partial x^2} = \frac{\partial c}{\partial t} \tag{4}$$

where c corresponds, in our case, to the oxygen concentration (that is proportional to partial pressure) and D the interdiffusion coefficient between oxygen and nitrogen. D is almost concentration independent and depends on temperature following the simple law [10]:

$$D(T) = D(T_{RT})\left(\frac{T}{T_{RT}}\right)^{3/2} \tag{5}$$

where $D(T_{RT}) = 0.181 \times 10^{-4}$ m^2 s^{-1}. Eq. (4) is also valid within the frame of reference that moves at the same velocity as the gas. Alternatively, one can transform it to the furnace's frame of reference. In this case, the gas moves at velocity, v_F, in the positive direction and Eq. (4) becomes

$$v_F\frac{\partial c}{\partial x} + D\frac{\partial^2 c}{\partial x^2} = \frac{\partial c}{\partial t} \tag{6}$$

If the furnace length is infinite, an initial abrupt front ($c = 1$ for $x < 0$ and $c = 0$ for $x > 0$) propagates following the analytic solution of Eq. (6) [10]:

$$c(x,t) = 0.5c_0\left(1 - \mathrm{erf}\frac{x - v_F t}{2\sqrt{Dt}}\right) \tag{7}$$

where erf(x) is the "error function". The centre of the front ($c(x,t) = 0.5c_0$) moves at velocity v_F. As we said before (Section 3), its average position is not modified by diffusion. However, this conclusion is not valid for the real case of a finite length furnace, L_F. At $x = L_F$, the gas increases its velocity because the diameter of the exhausting hose is much smaller than the furnace diameter. Consequently, Eq. (6) cannot be applied beyond $x = L_F$. One simplified way of including this reduction of section is by introducing a proper boundary condition. We assume that oxygen concentration is the same at the end of the furnace than at the beginning of the hose (continuity of $c(x)$):

$$c(x = L_F) = c(\text{hose}) \tag{8}$$

In addition, mass conservation implies a boundary condition involving the gradient of c:

$$A_F\left[c(L_F)v_F - D\left.\frac{\partial c}{\partial x}\right|_{L_F}\right] = A_H\left[c(\text{hose})v_H - D\left.\frac{\partial c}{\partial x}\right|_{\text{hose}}\right] \tag{9}$$

where A_F, A_H, v_F and v_H are the section's area and gas velocity of furnace and hose, respectively. In Eq. (9), oxygen transport includes two terms. One is simply due to the movement of the gas as a whole:

$$A_F c(L_F)v_F = A_H c(\text{hose})v_H = Qc(L_F) \tag{10}$$

The other one is due to diffusion and can be neglected on the side of the hose, where A_H and $\partial c/\partial x|_{\text{hose}}$ are much smaller than in the furnace. When the gas enters in the hose, any volume element elongates along the axial direction by a factor A_F/A_H. As a result, the concentration gradient will diminish by the same amount. So, the oxygen transport due to diffusion is, approximately $(A_F/A_H)^2$ times smaller on the side of the hose and, after introduction of Eq. (10), Eq. (9) can be simplified to

$$Qc(L_F) - D\left.\frac{\partial c}{\partial x}\right|_{L_F} = Qc(L_F) \tag{11}$$

which implies that the concentration gradient must be zero at the end of the furnace:

$$-D\left.\frac{\partial c}{\partial x}\right|_{L_F} = 0 \tag{12}$$

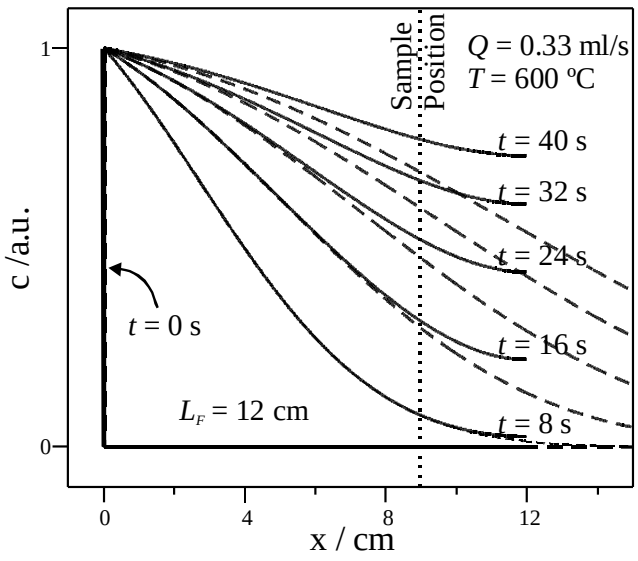

Fig. 6. Time evolution of the oxygen concentration profile calculated in the approximation of an infinite length (dashed curves) or finite length furnace, L_F (solid curves).

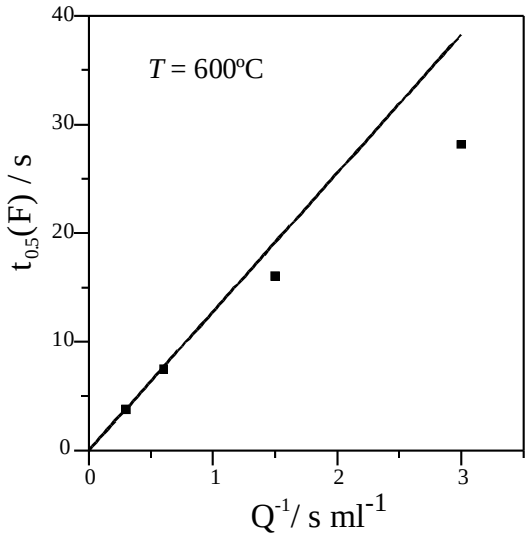

Fig. 7. Theoretical time delay, $t_{0.5}(F)$, as a function of gas flow rate, Q, by considering perfect thermalisation and by taking into account gas interdiffusion in a finite length furnace. The solid line corresponds to the predicted values without considering diffusion.

Now, the diffusion equation (Eq. (6)) can be solved numerically with the boundary condition of Eq. (12). The result for the smallest flow rate has been plotted in Fig. 6 altogether with the analytical solution corresponding to an infinite furnace. One can see that, in the realistic case (finite furnace) oxygen accumulates at the end of the furnace and causes its concentration to increase at any point and, in particular, at the sample's position. So, the time delay will be shorter than expected. The value of $t_{0.5}(F)$ has been plotted as a function of Q in Fig. 7, where complete thermalisation has been assumed. For comparison purposes, the straight line, which corresponds to the elementary solution of Eq. (1), has been included (Eq. (3)). We observed that axial diffusion has a noticeable effect at low flow rates, the effect on $t_{0.5}$ is contrary to that due to a lack of thermalisation. At high flow rates, the contribution of axial diffusion on $t_{0.5}$ is negligible.

6. Conclusions

Although the geometry and temperature distribution of the furnace is quite complicated, the phenomena governing gas renewal have been explained in a semiquantitative way. In absence of gas interdiffusion and with perfect thermalisation, the front of oxygen would be abrupt and the time needed for oxygen to reach the sample would depend on gas flow rate and temperature, according to Eq. (1). At low flow rates, this time delay is shorter than expected because of the accumulation of oxygen occurring at the exit of the furnace. At higher flow rates, the time delay is longer than expected due to the lack of thermalisation. Hence, from a practical point of view, the time delay reduction that one would expect when flow rate is increased is lesser than expected, and besides there are thermalisation problems. This last point is much more critical when performing differential thermal analysis. An independent way of reducing the time delay, which would not produce this inconvenience, is to shorten the length of external hoses as much as possible.

Acknowledgements

This work was supported by the Spanish Programa Nacional de Materiales under contracts no. MAT99-569-C02-02 and MAT-2002-04236-C04-02. One of the authors (C. Rath) wishes to acknowledge the Ministerio de Ciencia y Tecnologia, Government of Spain, for support.

References

[1] M. Uematsu, H. Kageshima, K. Shiraishi, J. Appl. Phys. 89 (2001) 1948.
[2] T. Shimoo, F. Toyoda, K. Okamura, J. Mater. Sci. 35 (2000) 3301.
[3] Z. Zheng, R.E. Tressler, K.E. Spear, J. Electrochem. Soc. 137 (1990) 2812.
[4] R. Truttman, R. Riesen, G. Widmann, J. Therm. Anal. 47 (1996) 259.
[5] A. Atkinson, R.I. Taylor, A.E. Hughes, Phil. Mag. A 45 (1982) 823.
[6] J.R. Welty, C.E. Wicks, R.E. Wilson, Fundamentals of Momentum, Heat and Mass Transfer, Wiley, New York, 1984, Chapter 18.
[7] P. Roura, J. Fort, J. Saurina, Eur. J. Phys. 21 (2000) 95.
[8] W.M. Rohsenow, J.P. Hartnett, Y.I. Cho, Handbook of Heat Transfer, 3rd ed., McGraw-Hill, New York, 1998.
[9] J. Farjas, P. Roura, in press.
[10] J.R. Welty, C.E. Wicks, R.E. Wilson, Fundamentals of Momentum, Heat and Mass Transfer, Wiley, New York, 1984, Chapter 24.